Single Scattering Properties of Aggregates of Bullet Rosettes in Cirrus Cloud

J. Um and G M. McFarquhar
Department of Atmospheric Sciences
University of Illinois at Urbana-Champaign
Urbana, Illinois

Introduction

During spiral descents of the University of North Dakota Citation through cirrus of a non-convective origin over the Atmospheric Radiation Measurement (ARM) Program's Southern Great Plains (SGP) site during the 2000 Cloud Intensive Operations Period (IOP), aggregates of bullet rosettes (hereafter aggregates) were observed (Figure 1) using a Cloud Particle Imager (CPI) at temperatures between -15 and -50°C. Many of these aggregates consisted of clusters of 2 or more bullet rosettes attached together so that there was more than one point from which the component bullets emanated. Because of this, these clusters are said to have more than one local center of mass. These shapes differ from those of conventional crystal models used to compute single scattering properties of aggregates (e.g., Yang and Liou 1998). Here the single-scattering properties for idealized models describing these observed aggregates are computed using a ray-tracing code (Macke 1993; Macke et al. 1996) at six wavelengths. In addition, the impact of the single scattering properties on the solar radiation field is computed using a Monte Carlo radiative transfer code.

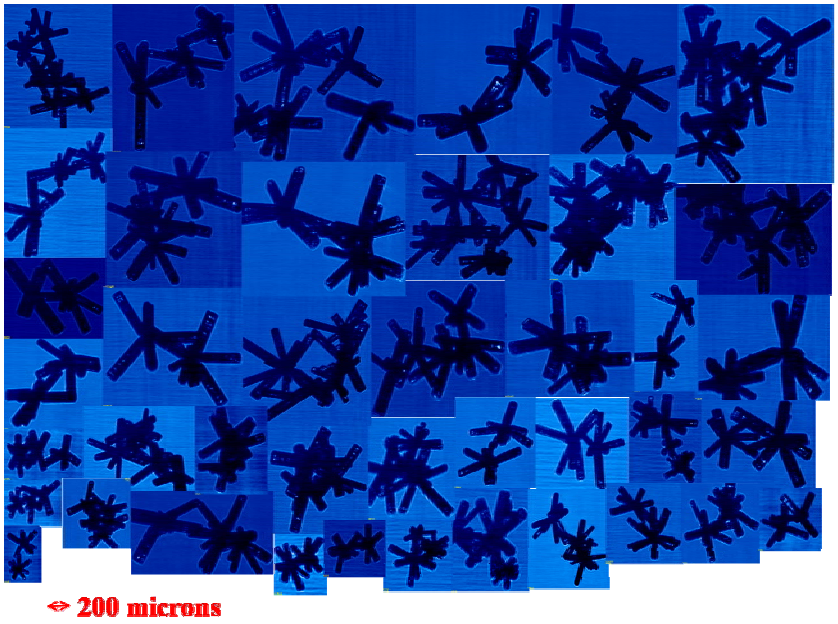

Figure 1. Aggregates imaged by CPI During 2000 Cloud IOP.

Methodology

Based on observed CPI images, the geometric shapes of ice crystals are described by the coordinates of the vertices in a three-dimensional Cartesian coordinate system. A plane equation defining a surface consists of three points in that surface. The geometric coordinates of aggregates were determined from the conjunction of three planes, which gives the point where the two bullet rosettes attach. At this conjunction, two bullet rosettes stick together without overlap.

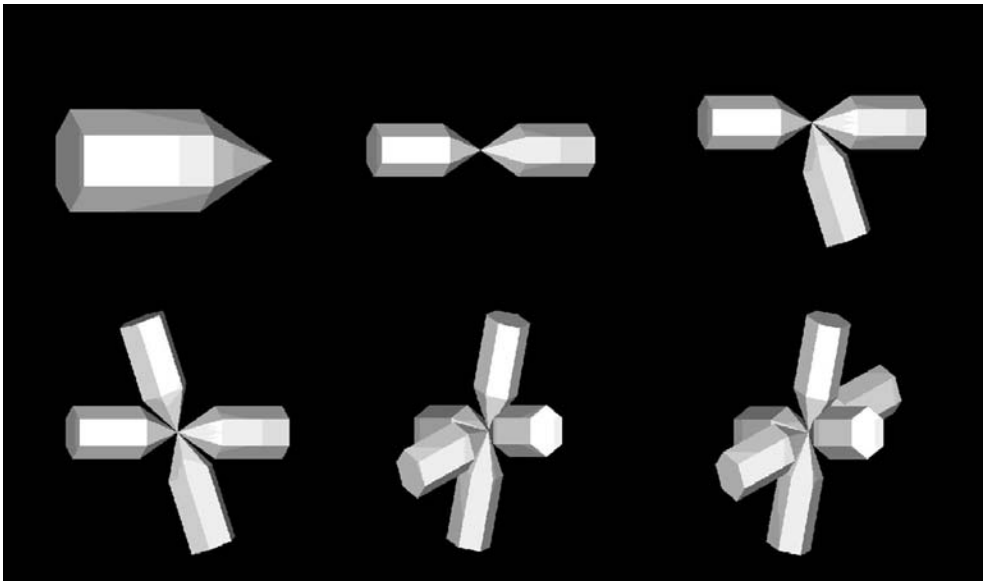

Figure 2. Idealized geometry of bullet and cluster of bullets. 1_bullet, 2_bullet, 3_bullet, 4_bullet, 5_bullet, and 6_bullet (1_br), from left top to clockwise.

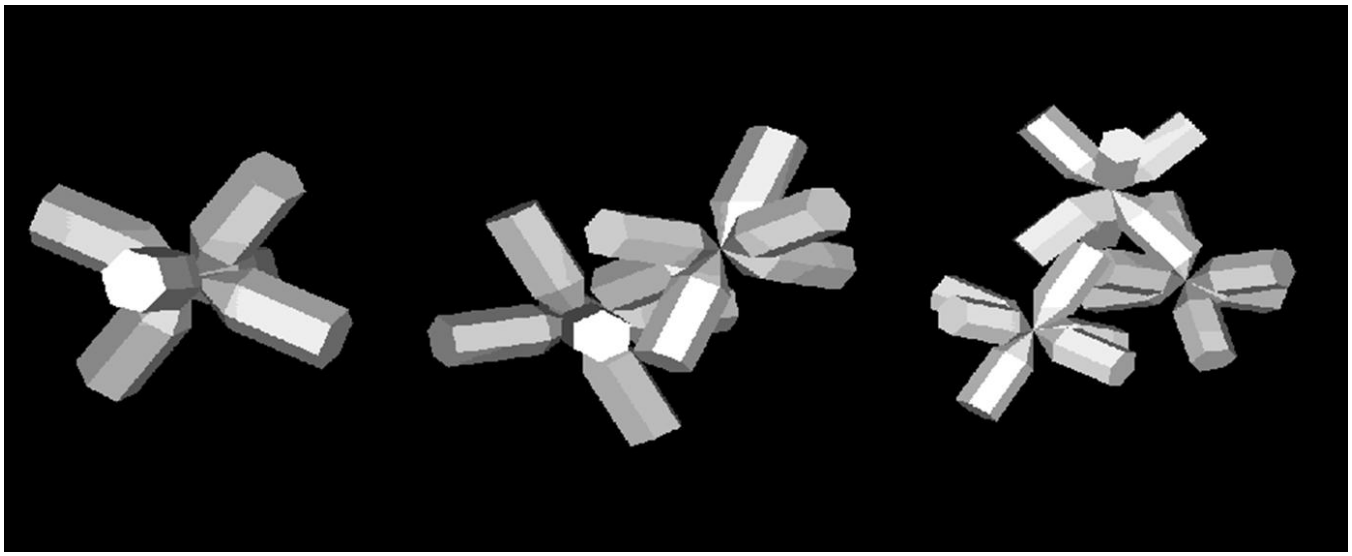

Figure 3. Idealized geometry of bullet rosette (1_br), 2_br, and 3_br.

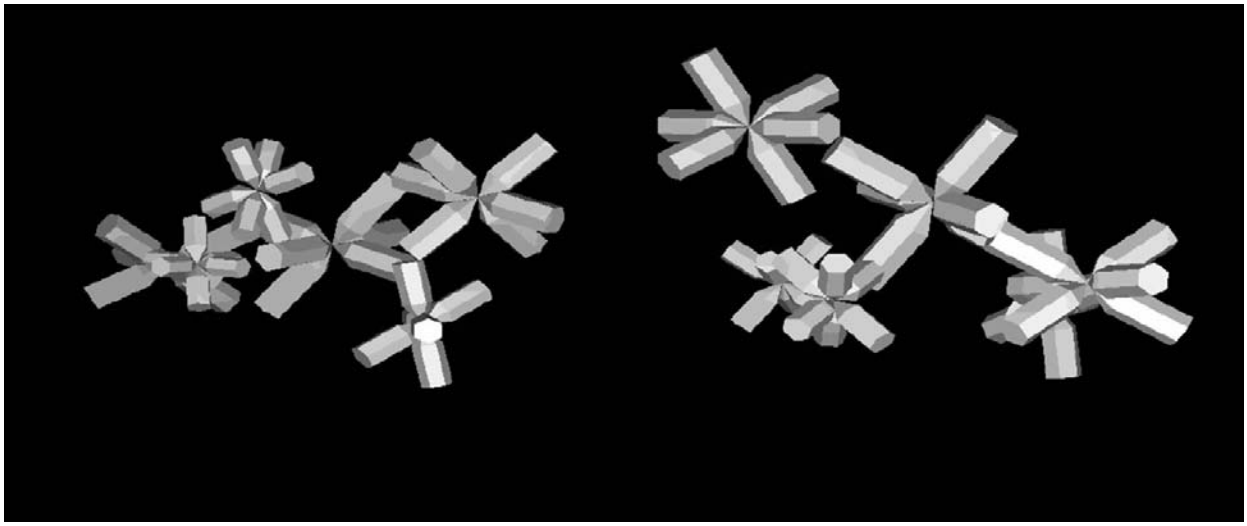

Figure 4. Examples of idealized geometry of aggregates (6_br).

In this paper, six types of bullet (Table 1) are used to determine the effects of bullet size and of aggregate shape on the single-scattering properties (i.e., phase function and asymmetry parameter). Henceforth, the notation y_name_x is used to describe the crystals used in the scattering computations, where y denotes the number of attached bullets or rosettes, x denotes the bullet or bullet rosette type, and name is the type of crystal considered (bullet or bullet rosette, denoted br). For the purpose of this study, a bullet rosette is assumed to consist of six bullets. For example, 3_br_2 indicates three bullet rosettes, each consisting of type 2 bullets, are attached together and 6_bullet_1 indicates that 6 type 1 bullets are attached together. In this paper, six types of bullet rosettes, attached together without overlap, are used to define the aggregates used for computing single-scattering properties. Table 2 shows the six different wavelengths at which the single-scattering properties are computed.

Table I. Geometry of Six Different Size Bullets.

Bullet Type	Length (L), μm	Radius (R), μm	Height (H), μm	Top Angle
Bullet_1	100	34.1605	55.6391	28°
Bullet_2	120	39.0325	63.5745	28°
Bullet_3	140	42.9685	69.9852	28°
Bullet_4	160	45.9685	74.8715	28°
Bullet_5	180	48.0325	78.2333	28°
Bullet_6	200	49.1605	80.0705	28°

Table II. Wavelengths, real and imaginary part of refractive index (Warren 1984).

Wavelength (μm)	m_r	m_i
0.47	1.3145	1.550 E-09
0.55	1.3110	3.110 E-09
1.24	1.2972	1.220 E-05
1.38	1.2943	1.580 E-05
1.65	1.2878	2.410 E-04
2.13	1.2674	5.650 E-04

Results

Size Effects

To calculate the size effects on the single scattering properties, six different sizes of bullet are considered. An angle resolution of 0.5° is used for computing the phase function with the Monte Carlo code. Figure 5 shows how the scattering phase function P_{11} varies with angle for the six different sizes of bullets used in this study. Each panel corresponds to different wavelength. General features are two well-known 22° and 46° halos caused by minimum deviation at 60° and 90° for ice prisms, broad 150° maxima, backward scattering, and an unusual peak at 9.5°. Even though this halo is an unusual, it has been observed (Neiman 1989).

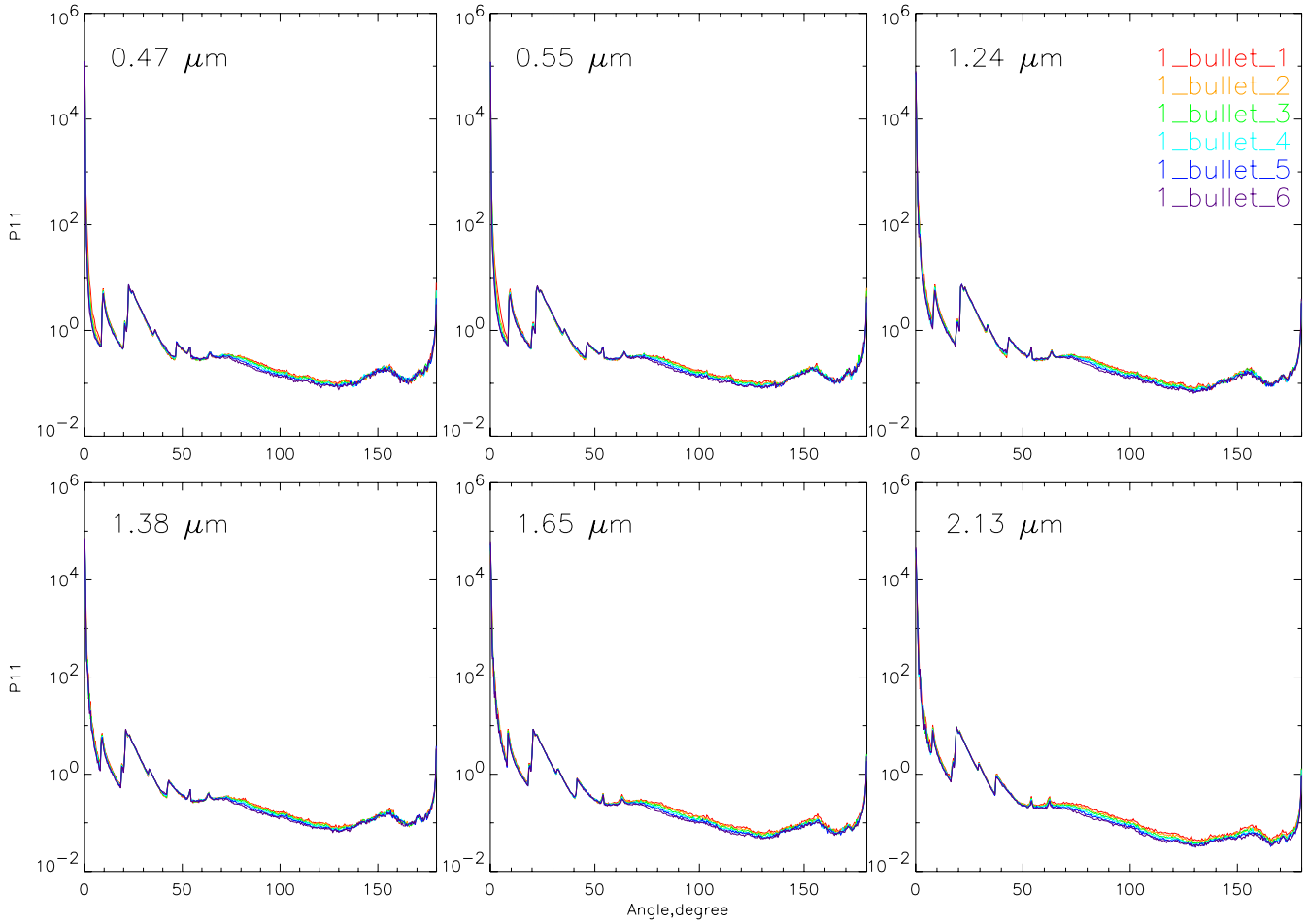

Figure 5. Phase functions of six different size bullets at six wavelengths.

For all six wavelengths, lateral and backward scattering (70° to 180°) decrease with bullet size. For the crystals used here, increasing size corresponds to a decreasing aspect ratio, the ratio between length and diameter of an ice crystal. The decreasing aspect ratio increases the amount of forward scattering and diminishes the lateral scattering. Furthermore, the increasing size implies stronger forward scattering

caused by diffraction, where the diffraction is parameterized by the Babinet's principle. The decrease of the lateral scattering is more significant with wavelength. This occurs because the imaginary part of the refractive index increases with wavelength so that absorption is more effective at longer wavelengths, and hence the lateral scattering is reduced by the absorption. Figure 6 is the same as Figure 5 except that the scattering properties are computed for bullet rosettes, instead of for bullets. The size effects for bullet rosettes are essentially the same as those for bullets. The only difference is that the lateral and backward scattering for bullet rosettes is smoother than for bullets.

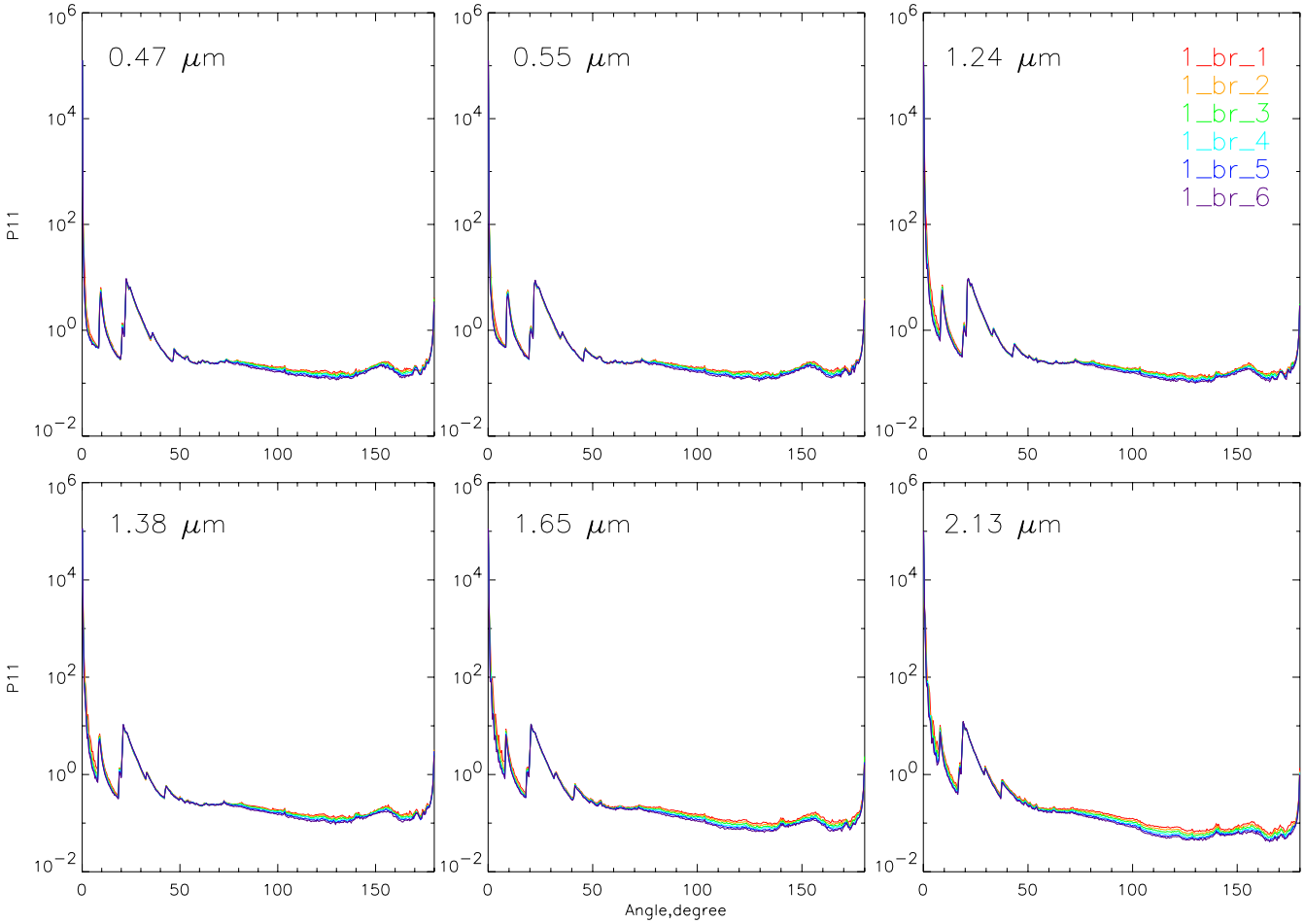

Figure 6. Phase functions of six different size bullet rosettes at six wavelengths.

Figure 7 summarizes the results, by showing that the asymmetry parameters increase with size for all six wavelengths. This is caused by more forward diffraction and less lateral scattering. It is also clearly seen that the asymmetry parameter of a bullet rosette is smaller than that of its component bullets, even though the bullet rosette is bigger than bullet. The reasons for this will be discussed at next section.

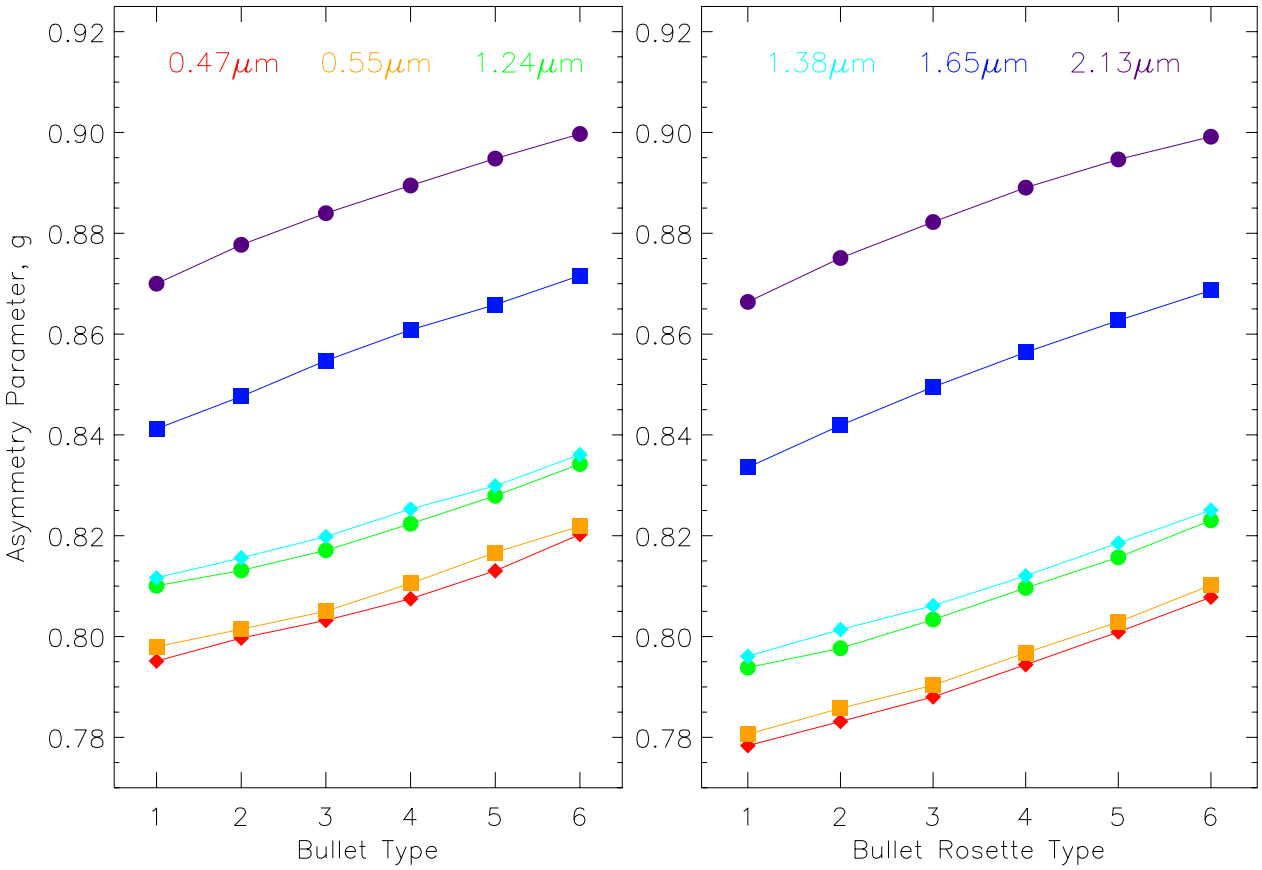

Figure 7. Asymmetry parameter of bullets and bullet rosettes with different size at six wavelengths.

Aggregation Effects

Phase functions for the bullet (1_bullet_6), cluster of bullet (2_bullet_6, 3_bullet_6, 4_bullet_6, and 5_bullet_6), a bullet rosette (1_br_6), and bullet rosette clusters (2_br_6 and 3_br_6) are shown in Figure 8. Aggregation has the effect of increasing the amount of lateral scattering, regardless of whether there are aggregates of bullets or of bullet rosettes. The more complex structures of aggregates means that more rays emerging from one branch of ice crystal can reenter into another branch, hence contributing to lateral scattering. The increasing lateral scattering due to the aggregation diminishes at near infrared wavelengths (e.g., 2.13 μm) because absorption at this wavelength reduces the number of lateral scattered rays. Therefore, the increased lateral scattering is canceled out by the absorption. In addition, small perturbations that appear due to the assumed simple geometry of ice crystals disappear for the more complex geometry of aggregates.

These trends are further shown in Figure 9 where the asymmetry parameter decreases with the number of bullets regardless of the geometry of the aggregate crystals. However, for 2.13 μm, the lateral scattering, which is mainly caused by several internal reflections, is weak and asymmetry parameters are almost constant regardless of the number of bullets as mentioned above. Therefore, only ice crystal size or type is important at this absorbing wavelength. An increase of asymmetry parameter with wavelength is also shown.

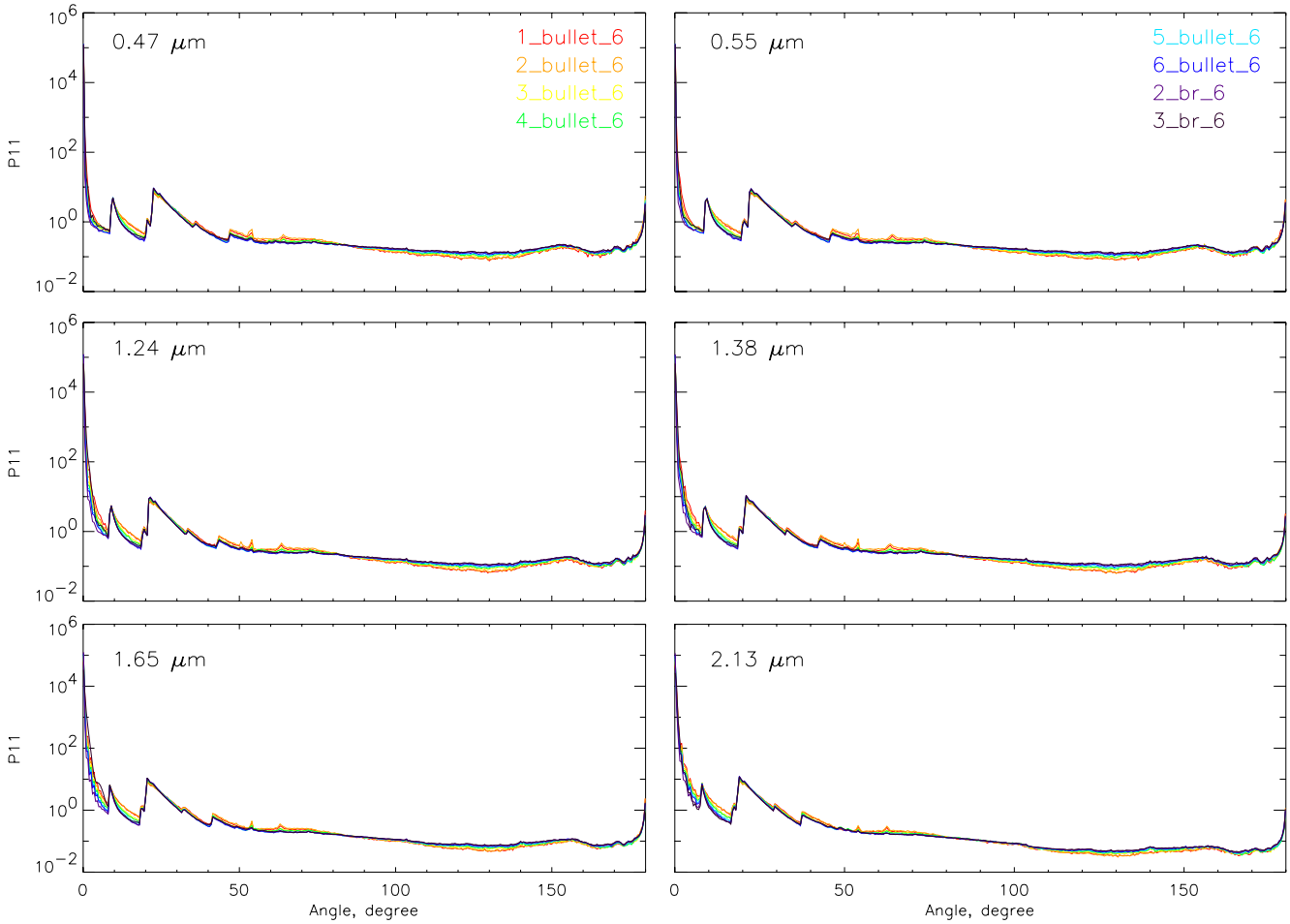

Figure 8. Phase functions of bullet and aggregates of bullets (only type 6 bullet) at six wavelengths.

Wavelength Dependency

As indicated in Table 2, the refractive index of an ice crystal depends on wavelength. The imaginary part of refractive index affects not only the Fresnel coefficients and the absorption of light but also the directions of the ray path within the ice crystal (Macke et al. 1996). Figure 10 illustrates the dependence of phase function on wavelength. As wavelength increases, the lateral and backward scattering are attenuated by absorption. Because the lateral and backward scattering is mainly caused by several internal reflections of rays, those rays must have a longer path length within the ice crystal, which in turn leads to more absorption of the lateral and backward scattering.

Another interesting feature is a halo shift. For example, 22° and 46° halos at non-absorbing wavelength (0.47 μm) shift to 20° and 39° at an absorbing wavelength (2.13 μm), respectively. However, the unusual halo (≈9.5°) has nearly the same peak angle at both wavelengths. The halo shift is a result of the absorption that occurs relating to the ray path length. The unusual halo is due to the pyramidal top of a bullet; on the other hand, 22° and 46° halos are as a result of a hexagonal column. The path length

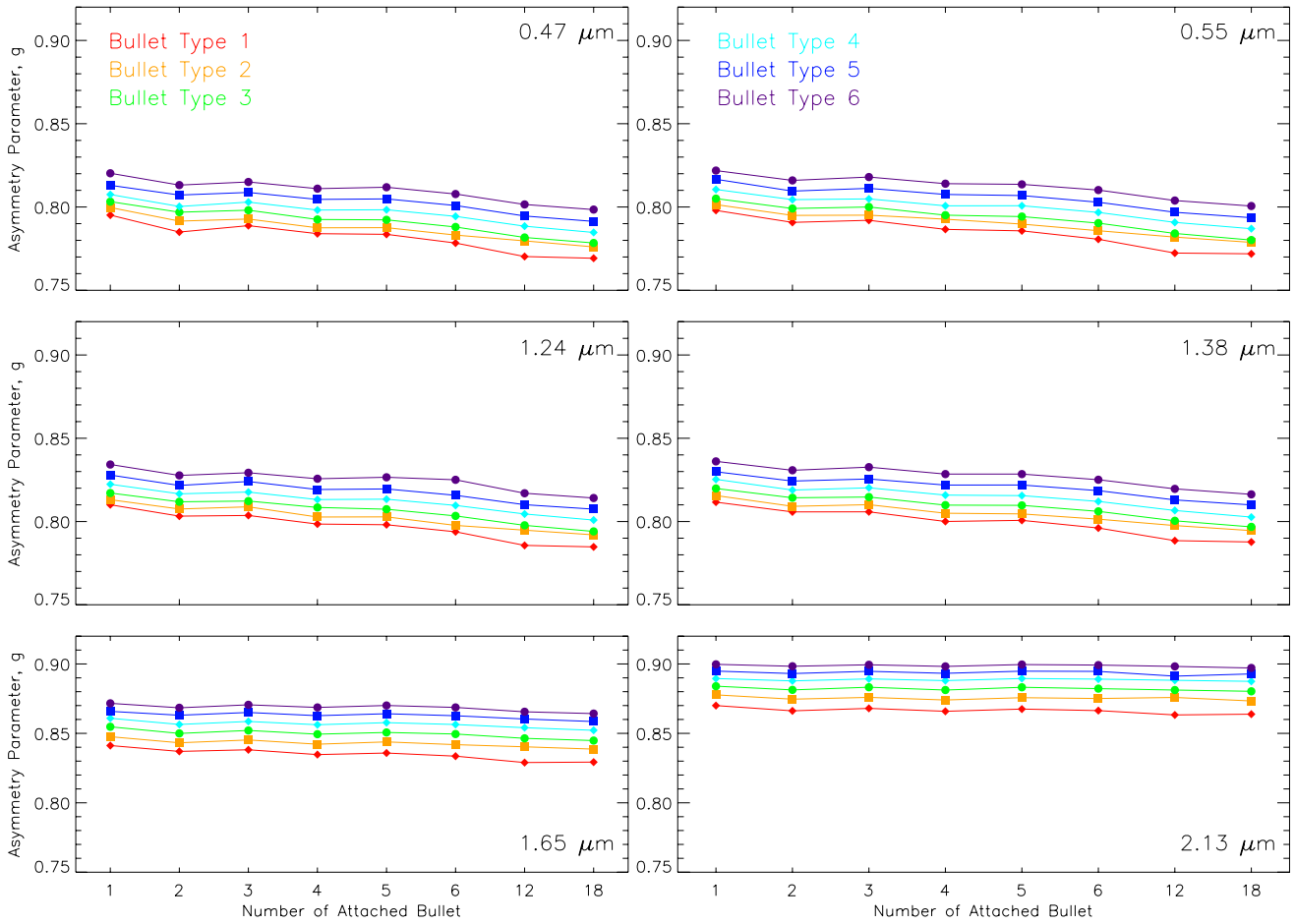

Figure 9. Variation of calculated asymmetry parameter with number of attached bullets (6 attached bullets is a bullet rosette, 12 attached bullets is two bullet rosettes attached, and 18 bullet attached is three bullet rosettes attached).

of rays, which produce the unusual halo, is shorter than that of 22°, and it is shorter than that of 46° halos. Therefore, in turn, the 46° halo shift is the largest, the 22° is next, and the unusual halo shift is the smallest. Although an ice crystal is almost non-absorbing object at visible wavelength (0.4 μm to 0.7 μm), it still absorbs some of rays and the halo shift can occur. Real halos, we frequently see in the sky, and artificial halos produced at laboratory or by theoretical calculation are somewhat different. The later is sharper than the former. Small deformations of ice crystal structure and ice crystal surface roughness are some of the reasons.

Aggregates of Bullet Rosettes

Aggregates (Figure 1) consist of several bullet rosettes. In this paper, a cluster of six different size bullet rosettes is regarded as an aggregate (6_br). Phase functions and asymmetry parameters for each component bullet rosette are shown in Figure 6 and 7. In Figure 11, the phase function and asymmetry

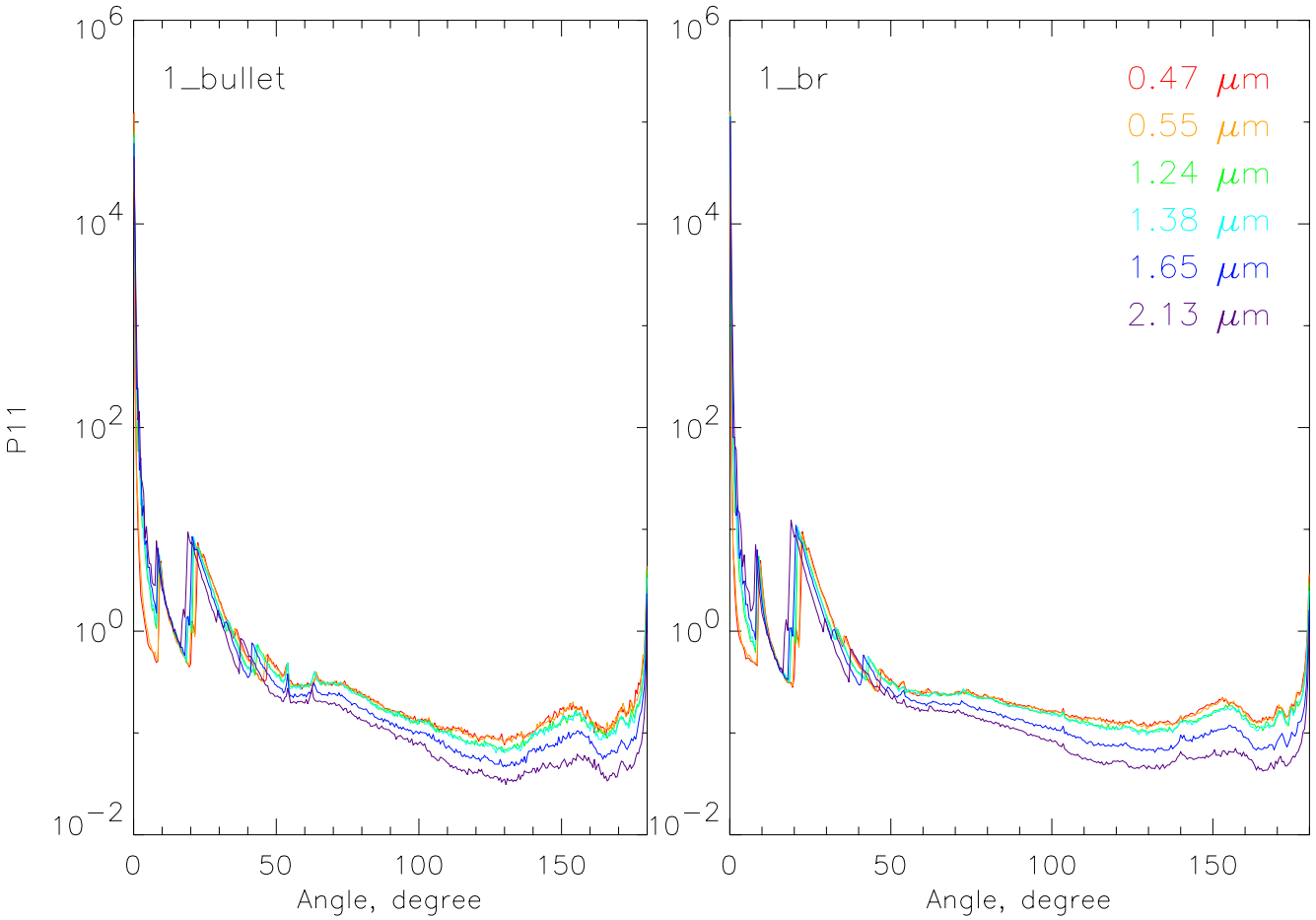

Figure 10. Phase functions of the bullet (1_bullet_6) and bullet rosette (1_br_6) at six wavelengths.

parameter of a single bullet rosette and that of aggregates are compared. Here, the single bullet rosette and the aggregates have the same cross section area to test whether a single bullet rosette can be used as a surrogate for aggregates.

The main characteristics of the aggregates' phase functions are similar to those of the single bullet rosette. The pronounced peaks (22° and 46°) still exist as previously shown by Macke (1993) and Iaquinta et al. (1995). However, some notable differences can be found in Figure 11, such as a one order of magnitude difference in the direct forward scattering, which is indicated by bars in Figure 11. The lateral and backward scattering of aggregates are also bigger than that of single bullet rosette, and this gap increases with wavelength due to the absorption. Hence, the asymmetry parameter of aggregates is smaller than that of single bullet rosettes even though the two ice crystals have the same cross section area. This result can be explained by ice crystal geometry. The geometry of aggregates is more complex than single bullet rosette. It implies that more rays emerging from one ice crystal can reenter into another adjacent ice crystal in complex geometry ice crystal. The rays undergoing several internal reflections scatter into lateral and backward directions. Therefore, the lateral and backward scattering readily occur within aggregates and help reduce the asymmetry parameter.

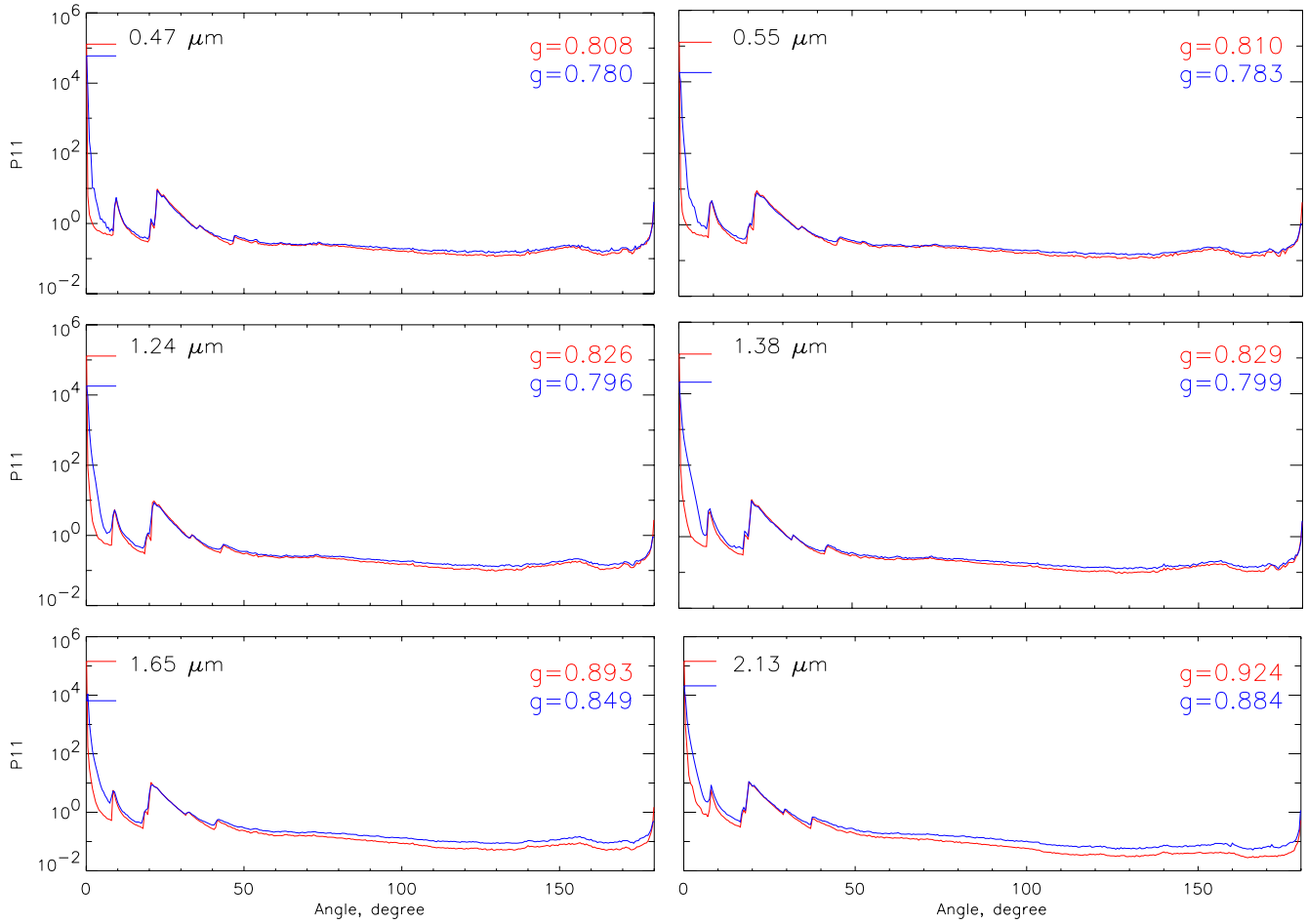

Figure 11. Phase function and asymmetry parameter of aggregates (blue, 6_br) and single bullet rosette (red, L= 370 μm). Each direct forward scattering is indicated by small bars.

Significance

To determine the importance of the difference between single scattering properties for single bullet rosettes and aggregates (6_br), the bidirectional reflectance function (BDRF) is calculated using Monte Carlo radiative transfer code (Macke et al. 1995) for both crystal geometries. Figure 12 shows the BDRF percentage differences as functions of optical depth and view zenith angle. Solar zenith angle (SZA) is 45° for all cases.

At 0.47, 0.55, 1.24, and 1.38 μm wavelengths, the largest difference is less than 20% and is found for nadir views and high optical depths. However, at 1.65 and 2.13 μm wavelengths, the difference can be as large as 50% and is found for high optical depths regardless of view zenith angle. The BRDF difference is only function of optical depth because of relatively strong absorption at these wavelengths. This has already been shown in Figure 8 and 9. In Figure 9, the asymmetry parameters are nearly constant regardless of the manner in which crystals are combined. Therefore, this may suggest a single bullet rosette can be a surrogate for aggregates at an absorbing wavelength in order to describe the phase

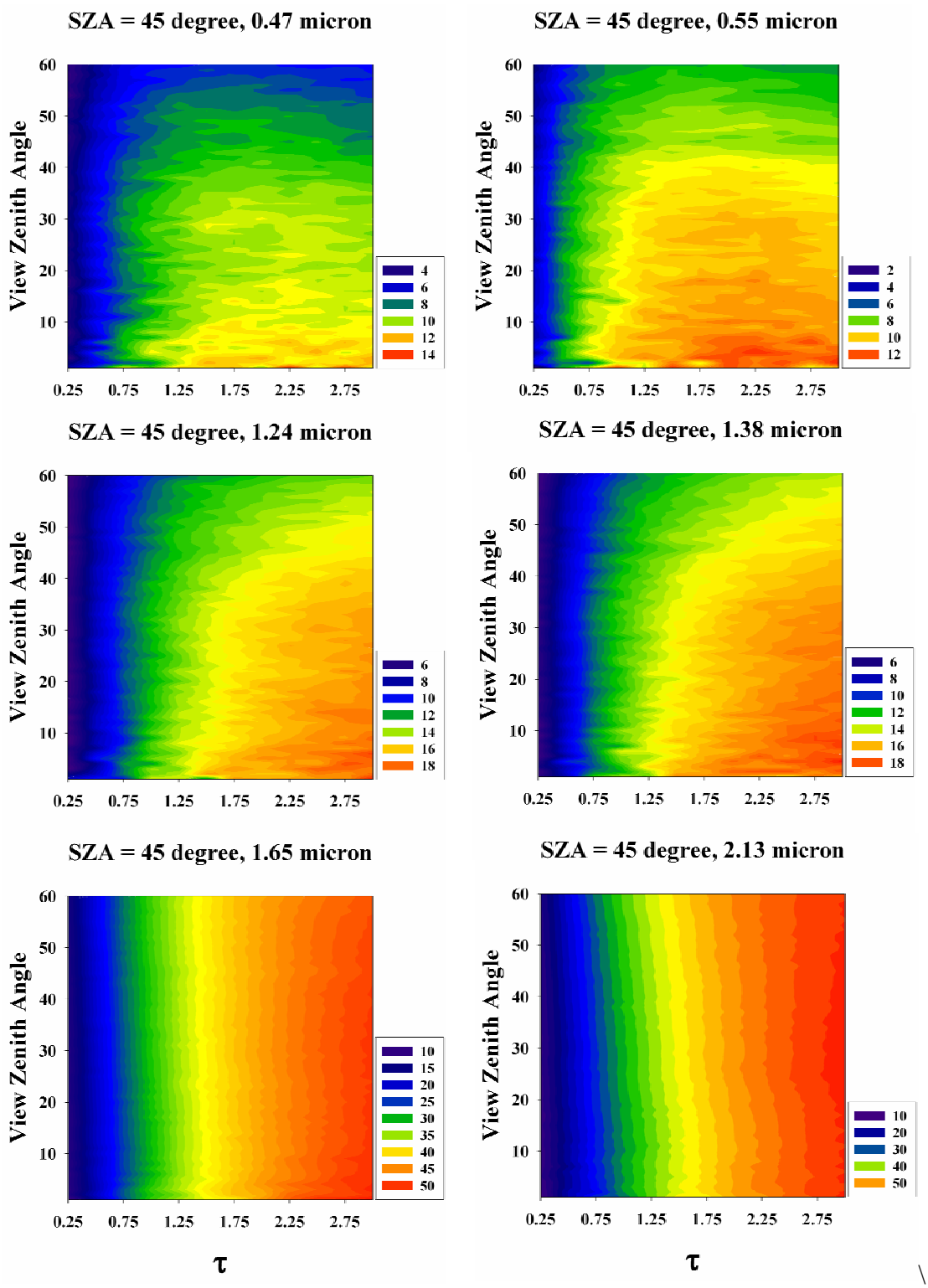

Figure 12. BRDF difference (%) between aggregates (6_br) and single bullet rosette (the same as Figure 11).

function and asymmetry parameter. However, with regards to the microphysical properties (e.g., cross section, size, ice water content), the use of a single bullet rosette as a surrogate for aggregates may be invalid.

Conclusions

Single scattering properties of bullets, bullet rosettes, and aggregates were calculated at six wavelengths. The difference between the single scattering properties of aggregates and those of its components are smaller than expected. Nevertheless, significant results are found as follows:

- The asymmetry parameter of aggregates decrease with the number of components
- Irregular particles scatter more light in the lateral direction than simple geometrical forms
- The phase functions of aggregates are similar to those of its components.
- A simple ice crystal can be used as a surrogate for aggregates at an absorbing wavelength
- Halo broadening can be explained due to the wavelength dependence of ice crystal absorption
- Accurate size or aspect ratio of ice crystals are required

Acknowledgements

This research was supported by the Department of Energy Atmospheric Radiation Measurement (ARM) program under grant number DE-FG03-02ER63337. Data were obtained from the ARM program sponsored by the U.S. Department of Energy, Office of Science, Office of Biological and Environmental Research, Environmental Sciences Divisions. We thank Andreas Macke for providing advice and the Monte Carlo codes used to simulate scattering.

Corresponding Author

Junshik Um, junum@atmos.uiuc.edu, (217) 333-9056

References

Iaquinta, J., H. Isaka, and P. Personne, 1995: Scattering phase function of bullet rosette ice crystals. *J. Atmos. Sci.*, **52**, 1401-1413.

Macke, A., 1993: Scattering of light by polyhedral ice crystals. *Appl. Opt.*, **32**, 2780-2788.

Macke, A., J. Muller and E. Rasche, 1996: Single scattering properties of atmospheric crystals. *J. Atmos. Sci.*, **53**, 2813-2825.

Macke, A., R. Clhopolsky, J. Muller, R. Stuhlmann and E. Raschke, 1995: A study of bidirectional reflectance functions for broken cloud fields over ocean. *Adv. Space res.*, **16**, 55-58.

Neiman, P. J., 1989: The Boulder, Colorado, concentric halo display of 21 July 1986. *Bull. Amer. Meteor. Soc.*, **70**, 258-264.

Warren, S. G., 1984: Optical constants of ice from the ultraviolet to the microwave. *Appl. Opt.*, **23**, 1206-1225.

Yang, P., and K. N. Liou, 1998: Single-scattering properties of complex ice crystals in terrestrial atmosphere. *Contrib. Atmos. Phys.*, **71**, 223-248.